Hydrodynamic condition and suspended sediment diffusion in the Yellow Sea and East China Sea

Li, Guangxue; Qiao, Lulu; Dong, Ping; Ma, Yanyan; Xu, Jishang; Liu, Shidong

Published in:
Journal of Geophysical Research: Oceans

DOI:
10.1002/2015JC011442

Publication date:
2016

Document Version
Publisher's PDF, also known as Version of record

AGU PUBLICATIONS

JGR

Journal of Geophysical Research: Oceans

RESEARCH ARTICLE

10.1002/2015JC011442

Hydrodynamic condition and suspended sediment diffusion in the Yellow Sea and East China Sea

Guangxue Li[1,2], Lulu Qiao[1,2], Ping Dong[1,3], Yanyan Ma[1,2], Jishang Xu[1,2], Shidong Liu[1], Yong Liu[1,2], Jianchao Li[1], Pin Li[4], Dong Ding[1,2], Nan Wang[1], Dada Olusegun A[1], and Ling Liu[1]

[1]College of Marine Geosciences, Ocean University of China, Qingdao, China, [2]Key Lab of Submarine Geosciences and Exploring Technique, Ocean University of China, Qingda, China, [3]School of Engineering, Physics and Mathematics, University of Dundee, Dundee, UK, [4]Department of Oceanography, Texas A&M University, College Station, Texas, USA

Key Points:
- Two dynamic sedimentary patterns driven by Asian monsoon and Kuroshio have been identified in ECSs
- Suspended sediment diffused by coastal current most come from Changjiang and Yellow River in ECSs
- Suspended sediments are trapped in the CWM and coastal current route

Supporting Information:
- Supporting Information S1
- Figure S1
- Figure S2
- Figure S3
- Figure S4
- Figure S5
- Figure S6
- Figure S7
- Figure S8

Correspondence to:
G. X. Li,
estuary@ouc.edu.cn;
L. L. Qiao,
qiaolulu126@sina.com

Citation:
Li, G., et al. (2016), Hydrodynamic condition and suspended sediment diffusion in the Yellow Sea and East China Sea, *J. Geophys. Res. Oceans*, *121*, doi:10.1002/2015JC011442.

Received 5 NOV 2015
Accepted 30 JUL 2016
Accepted article online 6 AUG 2016

Abstract Based on monthly averaged current, temperature, and salinity, we analyzed the changes of suspended sediment concentration (SSC) and the relationship with the warm current, coastal current, and cold water mass (CWM) in the East China Seas (ECSs). The result shows that the coastal current and surface diluted water are the route for transporting suspended sediment. The Kuroshio and its derived warm current branches play the important role of the continental shelf circulation system and control the diffusion of suspended sediment. High SSC has been mainly concentrated in coastal current and CWM. Two sedimentary dynamic patterns have been identified. The winter-half-year pattern lasts almost 7 months. The coastal currents off the Shandong Peninsula, northern Jiangsu, Zhejiang-Fujian coast are the main routes for diffusion and deposition of the suspended sediment from the Yellow River and Changjiang River. The summer-half-year pattern is characterized by the well-developed CWM. All CWMs have a unique function to trap suspended sediment under the thermocline due to weakening tidal current and residual current there. These CWMs in the Yellow Sea (YS) and north ECS are connected together. The layer above the thermocline is characterized by diluted water with low salinity, high temperature. Suspended sediment can be transported into the Okinawa Trough and the South Korea coast during this period. A strong eddy always occur nearby the *Kuroshio bend at* northeast Taiwan, which has promoted the exchange between the ECS shelf and Okinawa Trough, and the development of the shelf edge current and Taiwan warm current (TWC).

1. Introduction

The broad ECSs is an exciting area characterized by active land-ocean interaction and complicated sediment "source to sink" processes. A great deal of suspended sediment from the Yellow River and Changjiang River is deposited and diffused under the circulation system in the ECSs (Figure 1). The East Asian monsoon and the Kuroshio are considered as two key drivers for the circulation in the YS and ECS [*Li et al*., 2006, 2014]. The *Kuroshio* is a strongest current in the east ECSs, which flows northward along the west slope of the Okinawa Trough. Its annually averaged discharge can reach 23 Sv [1 Sv = 10^6 m^3 s^{-1}; *Ichikawa and Chaen*, 2000]. Its main current travels through the Tokara Strait to return to the Pacific Ocean. The Tsushima warm current still has a transport of 2–3 Sv into the Japan Sea [*Isobe et al*., 2002; *Teague et al*., 2002; *Takikawa et al*., 2005]. *Isobe and Beardsley* [2006] conducted a simulation that has indicated the importance of frontal wave of the *Kuroshio* in the matter exchange with the ECS. Under the influence of terrain, the Yellow Sea warm current (YSWC), Tsushima warm current and TWC have been formed due to the water climbing of the Kuroshio [*Yuan et al*., 2008; *Li et al*., 2009; *Yuan and Hsueh*, 2010; *Chen*, 2011; *Qiao et al*., 2011a]. Previously, *Uda* [1934] believed that the YSWC occurs in any season, while other researchers later thought that it does not exist in the summer [*Lie*, 1986; *Lie et al*., 2000, 2001; *Ma et al*., 2006]. *Lin et al*. [2011] for the first time systematically observed the change of the YSWC in the winter and believed that the factor driving the YSWC is a barotropic current. TWC appears obvious seasonal variation. Its velocity is faster in the summer and slower in the winter, which is mainly influenced by the seasonal variation of the Kuroshio and monsoon [*Su and Wang*, 1987]. *Chen and Wang* [2006] were the first to demonstrate that the Kuroshio climbs in northeast Taiwan and flows northwestward, leading to the TWC formation [*Chen*, 2011]. *Chang et al*. [2010] believed that the circulation of north Taiwan is shaped by the interaction between the strong Kuroshio and weak TWC.

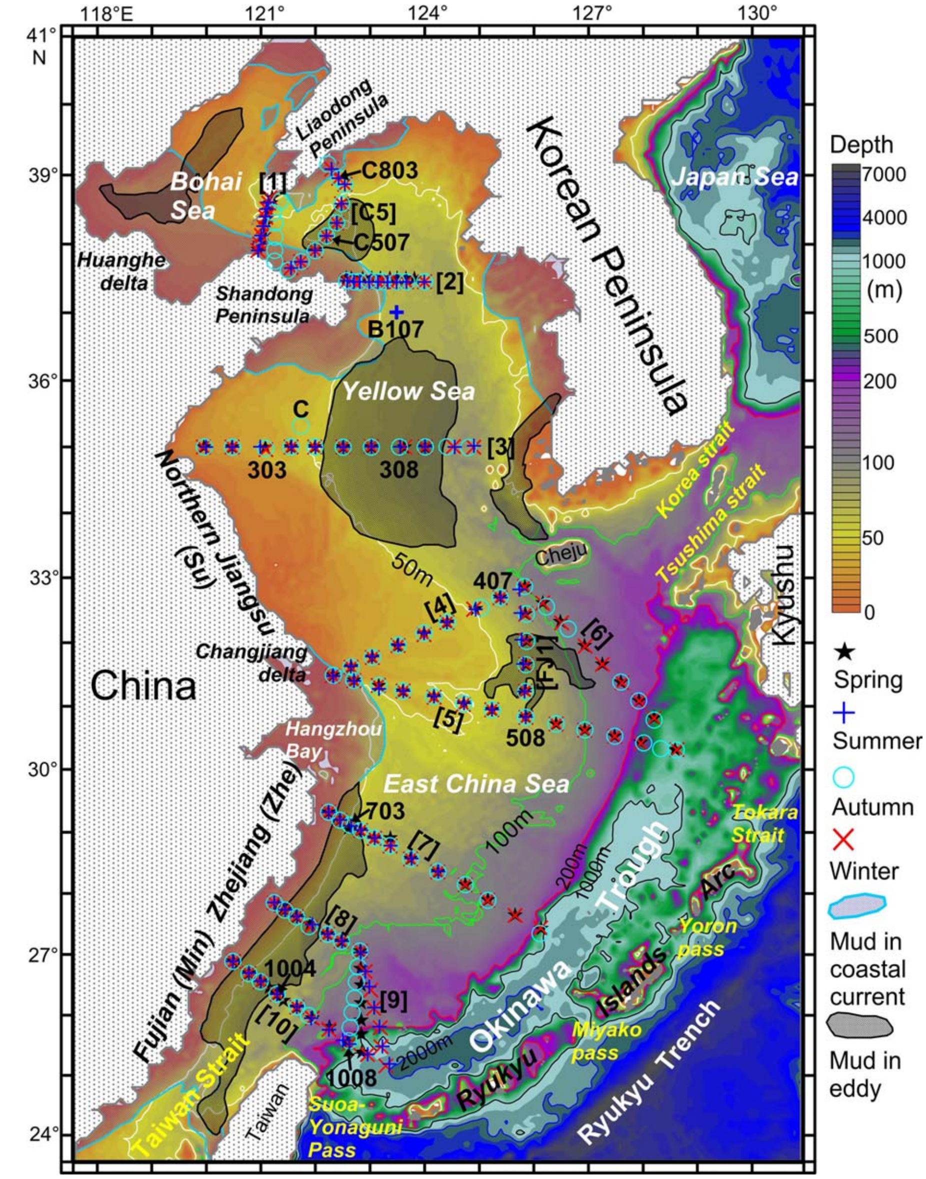

Figure 1. Topographic map and seasonal measured profiles in the East China Seas. Number in square bracket is the number of measurement section. Survey station with a number is a continuous measurement station. 50, 100, 200, 1000, and 2000 m on the vertical bar are water depth. The location of muddy area is based on *Li et al.* (2014).

The coastal current is characterized by low temperature, low salinity and high SSC, and seasonal change. It forms the circulation system in the ECSs together with the warm currents [*Liu et al*., 2007, *Yuan and Hsueh*, 2010]. The CWM in the ECSs is formed in the summer. *He et al*. [1959] had studied the characteristics and causes of the CWM in the YS. They believed that the CWM is formed in situ in the winter.

The modern circulation system in the ECSs was established after the last highstand sea level [*Liu et al*., 2010; *Li et al*., 2010, 2014]. Several mud areas were found in the continental shelf, forming the major deposit sinks [*Park et al*., 2000; *Yang et al*., 2003; *Chen and Zhu*, 2012]. In the west ECSs, large quantity of freshwater and sediment enter the sea from the Yellow River and Changjiang River [*Lie et al*., 2003; *Wang et al*., 2011]. The annual sediment load from the Changjiang River and the Yellow River accounts for 10% of the world total load [*Milliman and Meade*, 1983], and 92.4% of total river load into the ECSs. The sediment, besides accumulated in the delta, diffuses to the wide continental shelf in the form of suspension load. Under the influence of East Asian monsoon, an active deposition system in the ECSs has been built as a result of interaction among the YSCC and YSWC, Zhejiang-Fujian coastal current (ZMCC), and TWC [*Chang and Isobe*, 2003; *Liu*

Table 1. Time Periods for the Seasonal Profiling

Profile No.	Winter	Spring	Summer	Autumn
[1]	6–8 Jan 2007	18 May 2009	23 Jul 2006	21–22 Oct 2007
[c5]	4–5 Jan 2007	/	25–31 Jul 2006	14–17 Oct 2007
[2]	10–16 Jan 2007	17 May 2009	4 Aug 2006	24 Oct 2007
[3]	12–13 Feb 2007	16 May 2009	14–15 Jul 2006	22–24 Nov 2007
[4]	9–10 Feb 2007	13 May 2009	10–11 Jul 2006	20–22 Nov 2007
[5]	23–25 Jan 2007	30 Apr, 10–11 May 2009	6–10 Jul 2006	3–5 Nov 2007
[FJ1]	29 Jan 2007	12 May 2009	11–12 Jul 2006	7 Nov 2007
[6]	26–29 Jan 2007	29–30 Apr 2009	/	5–7 Nov 2007
[7]	1–3 Feb 2007	1–3 May 2009	4–6 Jul 2006	18–19 Nov 2007
[8]	8 Feb 2007	3 May 2009	3 Jul 2006	16–17 Nov 2007
[9]	3–4 Feb 2007	4 May 2009	2 Jul 2006	13 Nov 2007
[10]	4–7 Feb 2007	4–7 May 2009	28–30 Jun, 1 Jul 2006	14–16 Nov 2007

et al., 2007; *Yuan and Hsueh*, 2010]. These mud areas (Figure 1) are related to the circulation system [*Zhu and Chang*, 2000]. The mud in the center of south YS occupy a largest area [*Li et al.*, 2014] with a sedimentary quantity of 3.6×10^{11} t since the Holocene [*Wang et al.*, 2014]. The suspended sediment from the Yellow River, Changjiang River, and the old Yellow River Delta in north Jiangsu is the majority of this muddy body [*Dong et al.*, 2011; *Wang et al.*, 2011]. *Saito et al.* [1999] concluded that each year 2.2×10^{8} t of the suspended sediment is diffused off the old Yellow River delta. *Yuan et al.* [2008] studied the diffusion of surface suspended sediment, and found that the suspended sediment from north Jiangsu coast is diffused mainly in the winter-half-year to as far as the mud area off the South Korea coast. *Lim et al.* [2007] investigated the deposition rate and demonstrated that the Korean rivers are insufficient in supplying the quantity of the muddy body off the South Korea coast. They concluded that the YSWC is involved in the transport of river matter from China coast toward northeast. The mud zone along the ZMCC has the largest volume. Since the Holocene, the quantity of sediment there has reached 5.4×10^{11} t and these sediments are mainly from the Changjiang River [*Liu et al.*, 2006, 2007; *Dong et al.*, 2011; *Xu et al.*, 2012] and can diffuse to as far as the Taiwan strait [*Huh et al.*, 2011].

In summary, some important processes of the ECSs on hydrodynamic condition, suspended sediment diffusion, and deposition have been studied by previous papers based on survey data in single season and limited areas. But, systemic knowledge on the seasonal deposition processes is lacking in whole ECSs. We had designed 12 profiles to be measured for four seasonal months on the ECSs (Figure 1) after overcoming finance and diplomacy difficulties. In the next section, data and methods for explaining data collection are presented, followed by the results of the evolution of circulation and suspended sediment diffusion in YS and ECS for four surveys in section 3, and discussion on two patterns of suspended sediment diffusion in section 4. Conclusions from the study will be given in section 5.

2. Data and Methods

2.1. Survey Data

The ship of Dongfanghong No. 2, the Ocean University of China, had carried out this project. Between 2006 and 2009, four surveys were finished (Table 1) with repeated measurements along 12 profiles. Each profile had a number of measured stations (Figure 1). Each station was measured within 20 min. The letters W, C, S, and F before the station name showed in winter, spring, summer, and autumn, respectively. A CTD analyzer, called Seabird 911Plus, was used to measure the water depth, temperature, salinity, and turbidity (supporting information Table S1). The layer spacing of CTD measurement was 1 m. Water samples for SSC were also collected from different water layer using the CTD bottles.

During the survey, 19 stations were selected to do continuous observation for 13 or 25 h on current, temperature, salinity, turbidity, and SSC, mostly at an interval of 1 h. Current velocity and direction were determined using acoustic Doppler current profilers (LADCP) at interval of 1 h. The current data were calibrated based on sound velocity bottom tracking information [*Fischer and Martin*, 1993; *Martin*, 2002; *Xiong et al.*, 2003; *Xie et al.*, 2009]. The daily average residual current at each continuous station was calculated by removing the periodic tidal signals.

The CTD analyzer had 12 sampling bottles. Water samples of 3–7 layers were taken at each station from sea surface to bottom. The water was filtrated using membranes with pore size of 0.45 μm and the samples left on the filters were washed, diluted, dried, and weighted with electronic balance with a precision of 1/100,000 g. Finally, the SSC was calculated.

2.2. Hydrological Background Data

In addition, we also collected and analyzed temperature and salinity data since 1930 in the study area. These data were mainly from the Tianjin International Ocean information Center. First, the quality of data is checked to remove any coordinate errors and anomaly stations. Then, an objective analysis method [*Barnes*, 1964, 1973] has been used to deal with the data. Four monthly averaged data (supporting information Figures S1, S3, S5, and S7, January, April, July, and October, respectively) have been finally obtained as the seasonal background in the ECSs.

HYCOM/NCODA reanalysis data are composed of the 1/12° global HYbrid Coordinate Ocean Model (HYCOM) and the Navy Coupled Ocean Data Assimilation (NCODA) system (http://hycom.org/dataserver/glb-reanalysis). Climatologically monthly averaged currents (supporting information Figures S2, S4, S6, and S8) in January, April, July, and November from 1998 to 2007, respectively, were derived from HYCOM/NCODA data.

3. Results

The distribution of monthly averaged temperature, salinity, and current is shown in supporting information Figures S1–S8. It is evident that there were clear seasonal changes in the coastal current, warm current, and CWM in the ECSs. We have compared the seasonal monthly averaged changes in the temperature, salinity, and current with our measured profiles in different year. The result shows that our four measurements (Table 1) are coincided with four monthly averaged changes on current systems and water masses, and is of seasonal representative.

3.1. Winter in 2007 (Figures 2 and 3 and Supporting Information Figures S1 and S2)

3.1.1. Yellow Sea

The YS was in the north of profile [4]. The YSWC intruding the YS near Cheju Island was clearly shown as higher temperature and salinity zones on the west side of profile [4]. Its residue reached the north YS with the higher temperature and salinity centers in the profiles. The warm water was even visible on profile [1] of the Bohai Strait through the temperature and salinity isolines. From profile [3], the YSWC intruded the YS mainly in the bottom layer (supporting information Figure S2b), and then affected the surface layer. It is consistent with some of our earlier results [*Li et al*., 2006]. On the profiles, the coastal currents close to the land appeared clearer with low temperature and salinity. There were two centers with low temperature and salinity on profile [4]. The coastal current near W501 was from the Changjiang River estuary. Another one near W404 could be extended from the coastal current off north Jiangsu (NSCC), which connects with the Shandong Peninsula coastal current (SPCC) in this season (supporting information Figure S2).

The SSC had positive relationship with coastal current and negative relationship with warm current. It was relatively higher in the left of profiles [1] and [2], reaching more than 40 mg/L, indicating that the SPCC from the Bohai Sea is carrying a lot of sediment from the modern Yellow River [*Zhou et al*., 2015]. The high SSC on the north profile [c5] also imply the impact from the Liaodong Peninsula coastal current. Profile [2] was, however, too short to identify the Korea coastal current on suspended sediment, which can be clearly found in supporting information Figure S2. Profile [3] had been measured across the south YS with strong coastal current on its west side but low SSC because it is far from the resuspension delta of old Yellow River of north Jiangsu [*Yuan et al*., 2008]. The SSC in the east profile [3] was relatively higher due to erosion by the strong current in the YS trough. Profile [4] located at the boundary of the YS and ECS. The SSC in the coastal current was very high, reaching more than 380 mg/L, with a narrow zone. The SSC from NSCC was also relatively high, particularly in the bottom layer at station W404 reaching up to 30 mg/L.

The continuous station C507 was setup in the middle of north YS (Figure 3a). Profile [C5] shows that it was located at the terminal of YSWC. The surface water within 5 m depth was desalinated with low salinity and temperature. The tidal current was diurnal with the maximum velocity of 20 cm/s. The residual current flowed at an average of 3.6 cm/s. Because of the influence of the YSWC, the SSC was low (less than 1.5 mg/L).

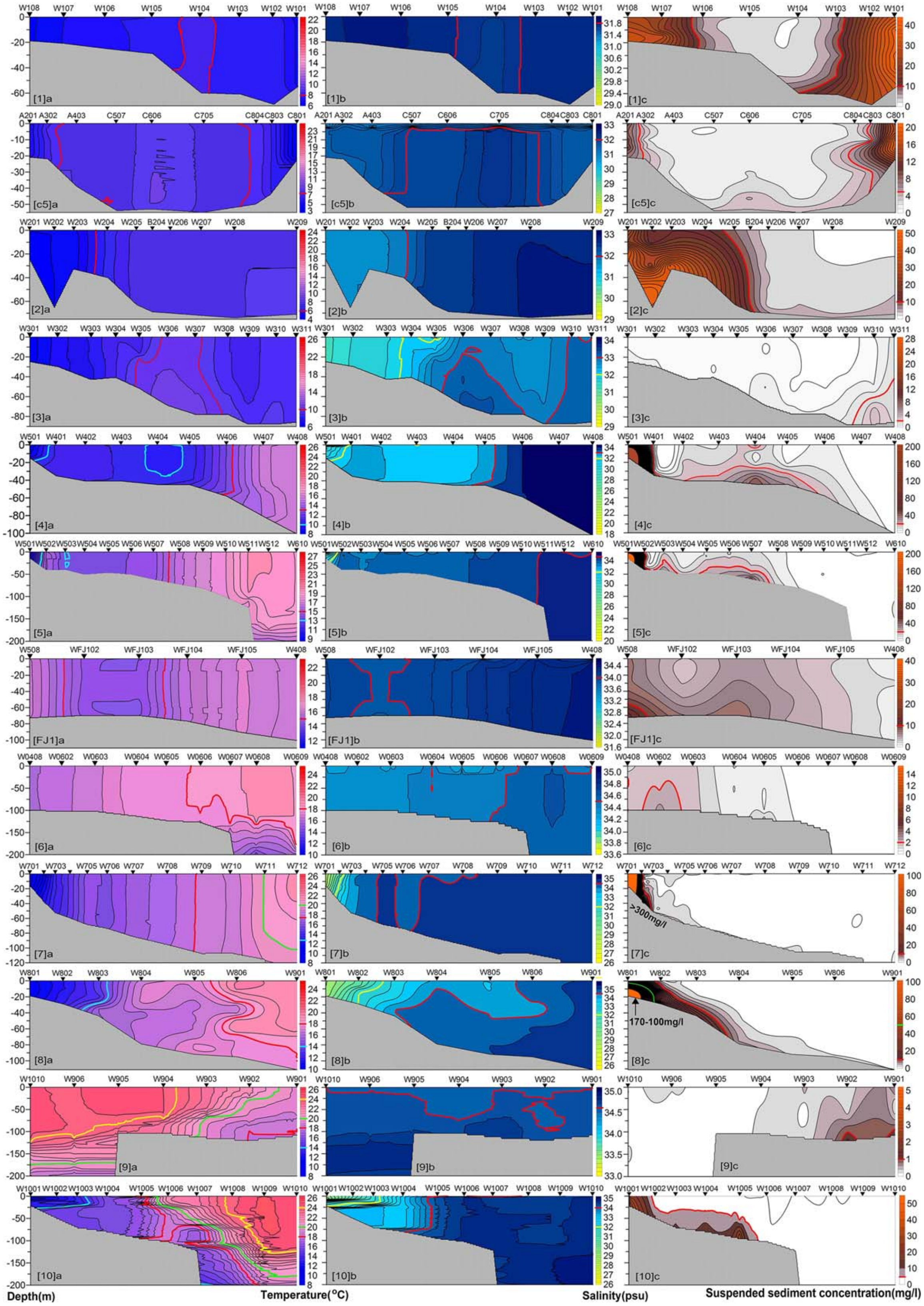

Figure 2. Observation profiles of the ECSs in winter, 2007. [1] to [10] denote the number of profiles. a, b, c, are temperature (°C), salinity (*psu*), and the SSC (mg/L), respectively. All the ordinates indicate the depth (m) of water.

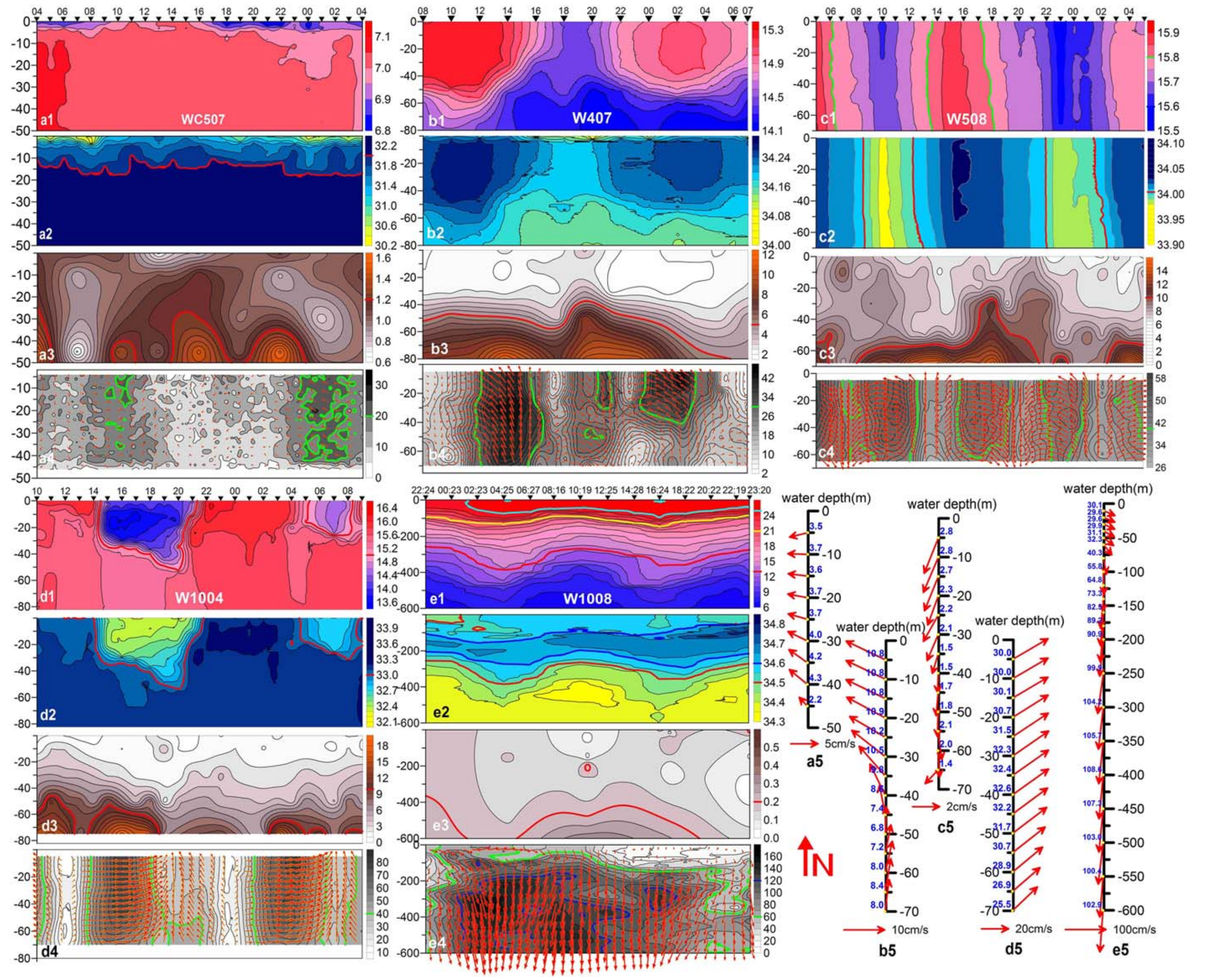

Figure 3. Continuous observation stations of the ECSs in winter, 2007. (a) Station WC507, observation beginning at 04:00, 13 January 2007 for 25 h at 1 h interval; a1–a5 are temperature (°C), salinity (*psu*), SSC (mg/L), current speed (cm/s), and residual current speed (cm/s). (b) Station W407, observation beginning at 08:00, 10 February 2007 for 25 h at 1 h interval. (c) Station W508, observation beginning at 05:09, 24 January 2007 for 25 h at 1 h interval. (d) station W1004, observation beginning at 10:06, 6 February 2007 for 25 h at 1 h interval. (e) Station W1008, observation beginning at 22:30, 4 February 2007 for 25 h at 1 h interval.

Continuous station W407 on profile [4] located near the start of the YSWC presented the irregular semidiurnal tide (Figure 3b). During flood, the current flowed northwest, and flowed southeast to transport cold water to the southeast during ebb. The residual current above 40 m depth reached 10.5 cm/s on average to the northwest in the same direction as the YSWC. The water below 40 m depth showed low temperature and salinity, but high SSC (>10 mg/L). The residual current reached an average speed of 7.8 cm/s to the north. It is clear that the bottom current on the west side was from the NSCC, suggesting that the NSCC could extend to the east of 125°E to impact on the mud area of Korea coast through the lower layer in winter (supporting information Figure S2b).

3.1.2. East China Sea

Profiles [5] and [6] were measured in the northern ECS. In the Okinawa Trough side, the northern extension of the Kuroshio occur [*Li et al.*, 2006]. From the two profiles, it can be seen that the impact of Kuroshio could reach a depth of 150 m (supporting information Figure S2). North Profile [FJ1] appeared higher temperature and salinity, resulting from the entering of the YSWC. According to the isotherm of profiles [9] and [10], the area with temperature > 24°C was the Kuroshio core. Because the Kuroshio comes from the open ocean, its

SSC is usually very low and barely detectable. Based on monthly averaged temperature and salinity (supporting information Figure S1), a weak TWC off the Zhejiang-Fujian coast occurred on profiles [8] and [10], which came mainly from climbing water of the Kuroshio (supporting information Figure S2b). The TWC could extend to the Changjiang River estuary [*Li et al*., 2006; *Yuan and Hsueh*, 2010], and had been found in station W705, W502, and W402. It affected all water layers with low SSC due to the impact of TWC.

The NSCC continued to extend through profile [4] toward the ECS and the characteristics of low temperature, low salt, and high SSC could be seen along the stations W403 to W405. Station W508 appeared semidiurnal tide, where the SSC was observed in the lower layer. The residual current moved southward with an average speed of 2 cm/s, indicating that the suspended sediment was transported southward by the NSCC in the lower layer. The ZMCC occurred clearly on profiles [7], [8], and [10] with the low temperature and salinity, and high SSC of $>$300 mg/L. The zone influenced by the suspended sediment was basically consistent with that of coastal mud area (Figure 1). Continuous station W1004 was measured at the north of Taiwan Strait with semidiurnal tide feature. In the late ebb tide, the temperature and salinity in upper water were lower, suggesting that it was influenced by the ZMCC swing. Suspended sediment was mainly trapped in the lower layer and the SSC exceeded 10 mg/L. The residual current flowed northeast at whole water layer with an average velocity of 30 cm/s, which was coincided with the model current (supporting information Figure S2b).

Continuous station W1008 located at the Kuroshio bend, resulting in complicated temporal changes in temperature, salinity, and current. The residual current appeared complex at W1008, where the upper 75 m layer flowed southeastward with an average speed of 30 cm/s, the water in 75–200 m layer southward with an average speed of 71 cm/s, and the water in 200–600 m layer southwestward with an average speed of 104 cm/s. The speed increased gradually from top to bottom, and reached the maximum at 400 m depth. These phenomena indicate that there exist a stronger Kuroshio edge eddy for all seasons which has been proved by the model of HYCOM//NCODA. Temperature of profile [10] indicated that the water under the Kuroshio could climb up toward the shelf. This phenomenon was also reported by *Chern et al*. [1990].

3.2. Spring in 2009 (Figures 4 and 5 and Supporting Information Figures S3 and S4)

3.2.1. Yellow Sea

A prominent feature of the YS in spring occurred for stratification of the temperature and salinity. The temperature above 10 m water depth increased while the salinity decreased due to enhanced solar radiation and precipitation. The YSWC could be found between stations C305–307 on the profile [3] across the middle of south YS, where there was a thermocline in 10 m water depth. There are two cold eddies on both sides of the YSWC in profile [3]. These cold eddies occurring in profiles [1]–[4] indicated that the CWM would be gradually formed. The west cold eddy occurred with higher SSC in the bottom layer, suggesting the presence of NSCC. The NSCC reached stations C405–407 on profile [4] along the 50 m isobath marked clearly by low temperature and salinity. It transported higher SSC in the bottom layers, which exceeded 20 mg/L. In addition, the SSC in coastal area was relatively high like in the winter, confirming the previous observation by *Wang et al*. [2011]. The distribution of temperature, salinity, and current (supporting information Figures S3 and S4) shows that the SPCC and NSCC could be connected together in this month.

3.2.2. East China Sea

The profiles near the shelf edge were obviously influenced by the Kuroshio that presented high temperature and salinity, and very low SSC. In particular, the water under the Kuroshio climbed up toward the shelf on profile [8]–[10] in south ECS. As a result, lifting water with lower temperature and higher salinity was easily identified. This feature is consistent with the early observations [*Chen*, 2011]. The water in the top layer (above 75 m) in continuous station C1008 flowed northward and reached an average velocity of 46.6 cm/s with desalination. The water in 75–200 m depth flowed to west by north at 30 cm/s, and below 200 m flowed northwestward at 5.5cm/s. The direction of current in station C1008 changed vertically, which indicates that a strong eddy still occurred at the Kuroshio edge. Due to the water climbing from the Okinawa Trough, a weak CWM had been formed in the bottom of profile [10] at north Taiwan. Supporting information Figure S4 shows that a strong TWC from the Taiwan Strait and Kuroshio climbing in the northeast Taiwan extended to the Changjiang River estuary, and also appeared in profiles [7], [5], and [4].

There was still ZMCC with low temperature, low salinity, and high SSC. However, the SSC value was lower than in the winter. On profiles [7] and [8], the surface diluted water was extended to the middle shelf.

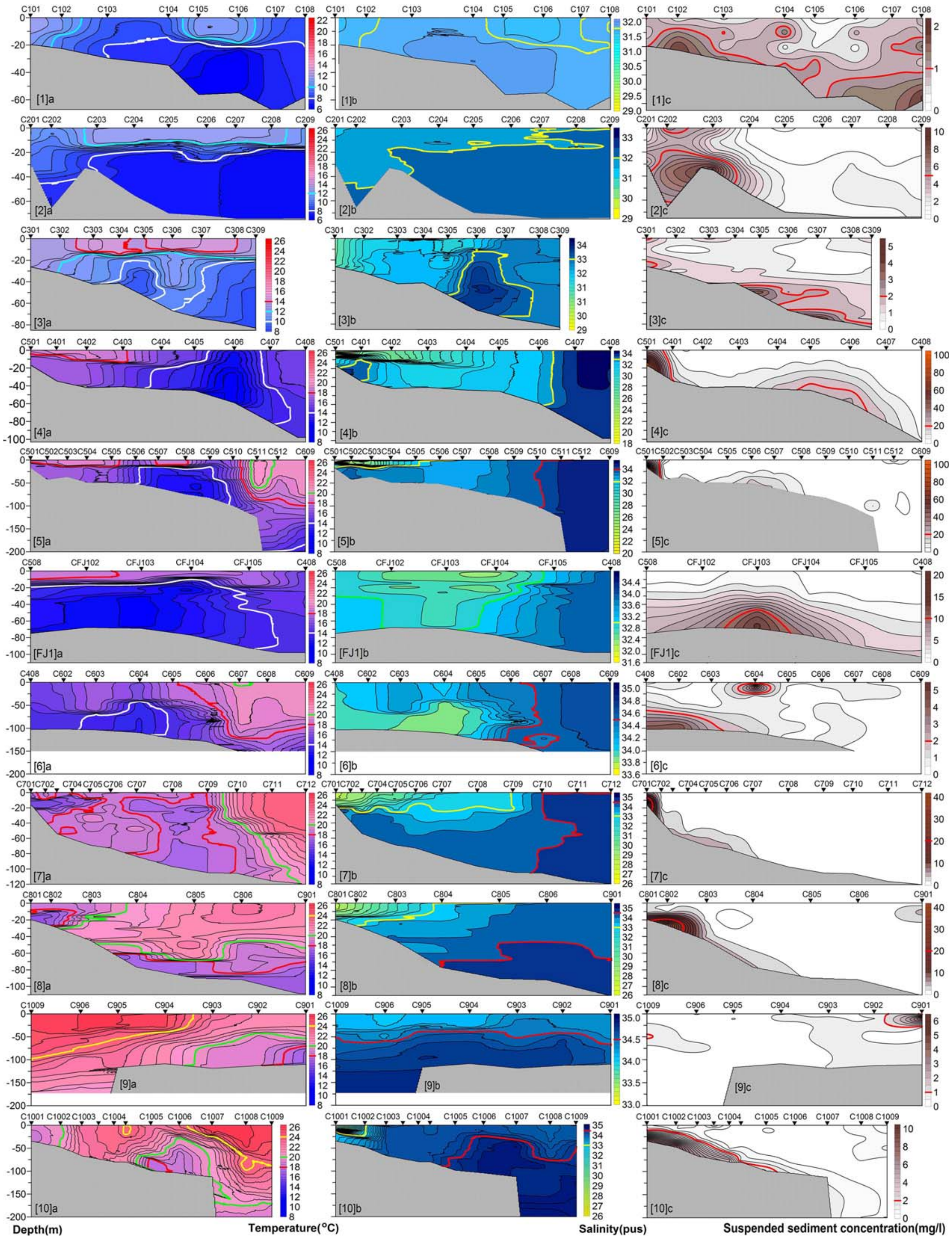

Figure 4. Observation profiles of the ECSs in spring, 2009. [1] to [10] denote the number of measurement profile; a, b, c, are temperature (°C), salinity (*psu*), and the SSC (mg/L).

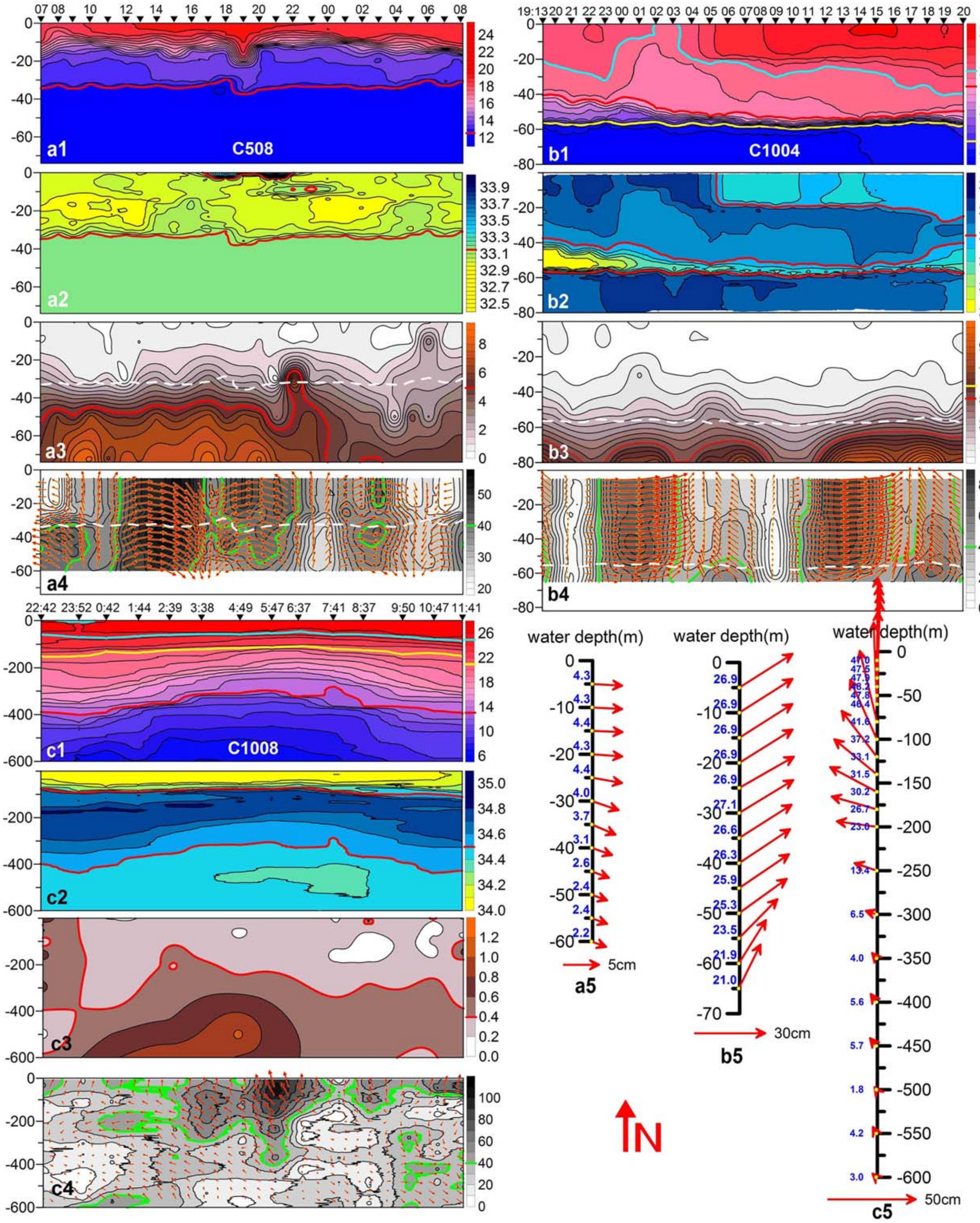

Figure 5. Continuous observation stations of the ECSs in spring, 2009. (a) Station C508, observation beginning at 07:00, 5 May 2009 for 25 h at 1 h interval; a1–a5 are temperature (°C), salinity (*psu*), SSC (mg/L), current speed (cm/s) on the profile and layered residual current speed (cm/s). (b) Station C1004, observation beginning at 07:13, 7 May 2009 for 25 h at 1 h interval; (c) station C1008, observation beginning at 22:42, 4 May 2009 for 13 h at 1 h interval. Broken line indicates location of the thermocline and halocline. The broken line indicates the top boundary of the CWM.

Continuous station W1004 showed that a thermocline at 55 m water depth occurred. There exist a semidiurnal tidal current. The residual current flowed northwestward at an average speed of 25.4 cm/s. Below 55 m water depth which there was a CWM to trap the suspended sediment, the SSC exceeded 5 mg/L (supporting information Figure 5b3). This might be resulted from the sediment transported by ZMCC during the ebb period. Salinity changes presented very unusual. Near 55 m water depth there was desalinated layer of 10–20 m thickness. Although the change value of salinity was small, it was clearly discernible. It is not clear what exactly had happen inside the thermocline, but at least it indicates that there was a permeation of the diluted water. From profile [10], it was clear that the bottom cool water under the thermocline of S1004 came from climbing water of Okinawa Trough.

The Changjiang diluted water had been developed in 10 m layer, and diffused to the middle shelf with high temperature and low salinity in profiles [4] and [5]. On profile [4], although it was connected to the NSCC, the Changjiang diluted water diffusion still was clear for salinity. Profile [FJ1] located in mud area of north ECS. The thermocline and CWM occurred with an internal temperature of less than 11.5°C. The CWM trapped higher SSC of more than 10 mg/L. Based on the distribution of temperature, salinity, current, and SSC, the suspended sediment had been transported from the NSCC through profile [4]. So we should see the impact of the NSCC in profiles [FJ1], [5], and [6]. Continuous station C508 within CWM showed that the residual current flowed eastward at an average speed of 3.5 cm/s. The thermocline had been developed at the depth of 20 m and the suspension sediment was trapped within the CWM.

3.3. Summer in 2006 (Figures 6 and 7 and Supporting Information Figures S5 and S6)

3.3.1. Yellow Sea

An obvious feature of the YS was the development of CWM in summer. The thermocline occurred about the depth of 20 m. The CWMs in the south and north YS had been connected together through the profile [2] (supporting information Figure S5). The core temperature of the CWM appeared from 6°C in north to 8°C in south. Due to the influence of coastal current, the SSC on the edge of the CWM presented relatively high. The CWM on profile [3] was well developed with powerful halocline and thermocline. Two CWM cores were similar to the spring occur on the profile [3] and a high salinity core in between. Therefore, it is believed that the CWM originated from the residual water of coastal current and cooled YSWC. This CWM extended to profiles [4] and [FJ1] containing high SSC in lower layer (>20 mg/L), which would be resulted from the diffusion of NSCC and Changjiang outflow (supporting information Figure S6). *Dong et al*. [2011] and *Qiao et al*. [2011b,2011c] believed that the weak current in the CWM facilitates the trapping of suspended sediment.

Continuous stations SC803 and SC507 located in the CWM of north YS with relatively deep thermocline (about 30 m). The SSC was concentrated in the bottom layer under the thermocline. The residual current of the CWM was weaker, the speed reached only 2–3 cm/s. Station SB107 located the northern CWM of south YS, where the suspended sediment was strictly controlled by thermocline and the residual current was very weak. Station S303 and C at the edge of the CWM appeared well-developed thermocline and halocline. The suspended sediment was also trapped by the CWM. Station S303 at the outer edge of the CWM indicated higher, southwest-bound residual current of 12 cm/s. Station C appeared the weak tidal current and very weak residual current.

3.3.2. East China Sea

The surface temperature over the entire YS and ECS exceeded 26°C due to solar radiation. The desalinated surface water could extend southward to the shelf edge and even the Taiwan Strait and Cheju Island due to the Changjiang outflow. ZMCC still transported southward the suspended sediment, and resulted in the relatively high SSC near the west profiles [7], [8], and [10]. Different from the spring and winter, the diluted water off the Zhejiang-Fujian coast occurred in the surface, while the cool water appeared in the bottom layer (supporting information Figure S5a3) where the suspended sediment was concentrated. On profile [7], two layers with high SSC could be seen in the lower cool water and upper diluted water. The temperature and salinity at the shelf edge of profiles [8], [9], and [10] had indicated that the bottom cool water just came from the climbing water from the Okinawa Trough. So, a CWM occurred in north Taiwan around station S1006, similar to the study by *Chern et al*. [1990]. Due to the diluted water transportation, the CWM trapped high SSC.

According to *Lie et al*. [2003], the Changjiang diluted water could reach near Cheju Island. It could effected the Tsushima strait based on the simulation results of *Chang and Isobe* [2003]. The NSCC flowed through the station S404 with low salinity and high SSC, extending to station SFJ102. The CWM of north ECS occurred in profile [FJ1]. Spatially, it was connected directly to the CWM of south YS through station S406.

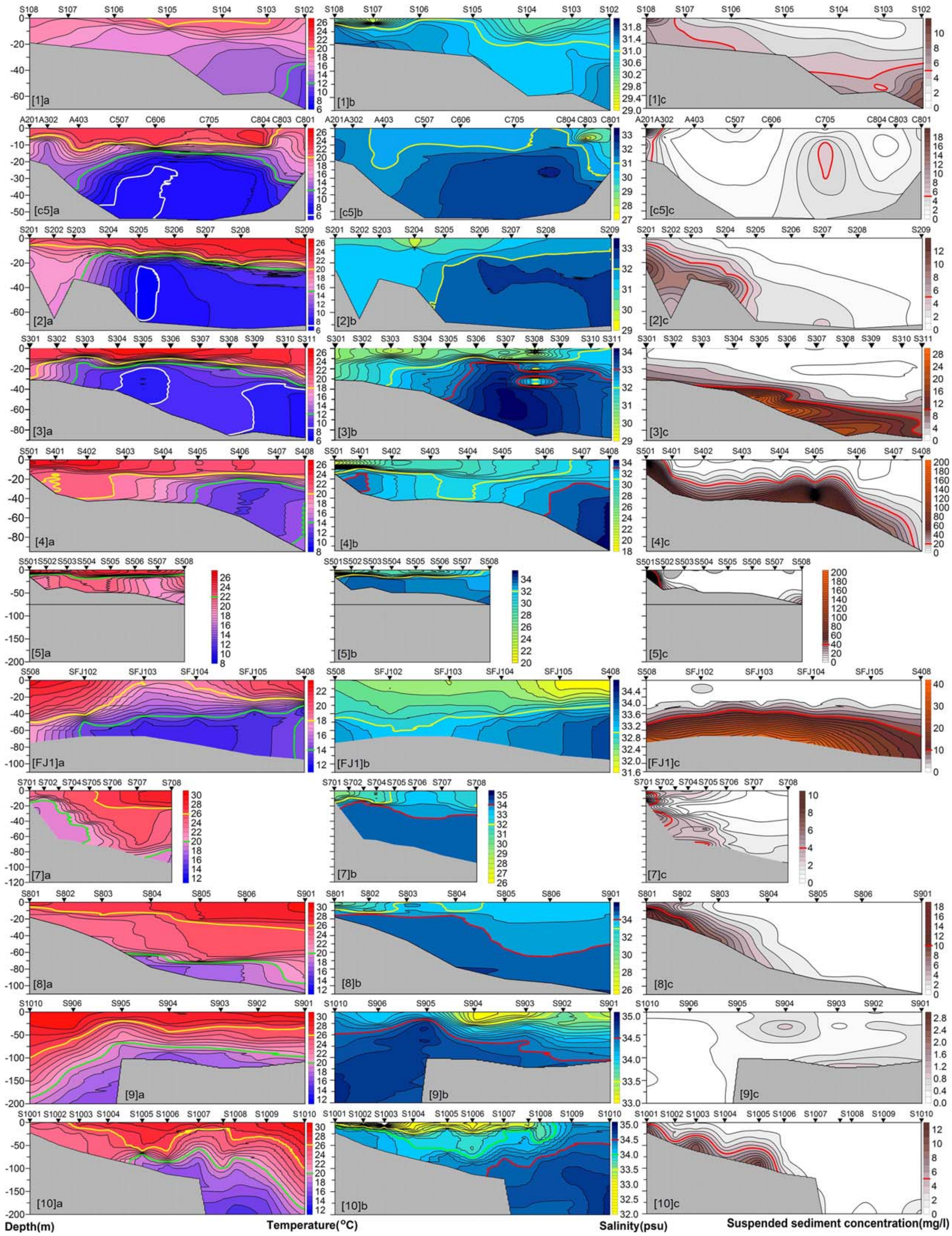

Figure 6. Observation profiles of the ECSs in summer, 2006. [1] to [10] denote the number of profiles; a, b, c, are temperature (°C), salinity (*psu*), and the SSC (mg/L).

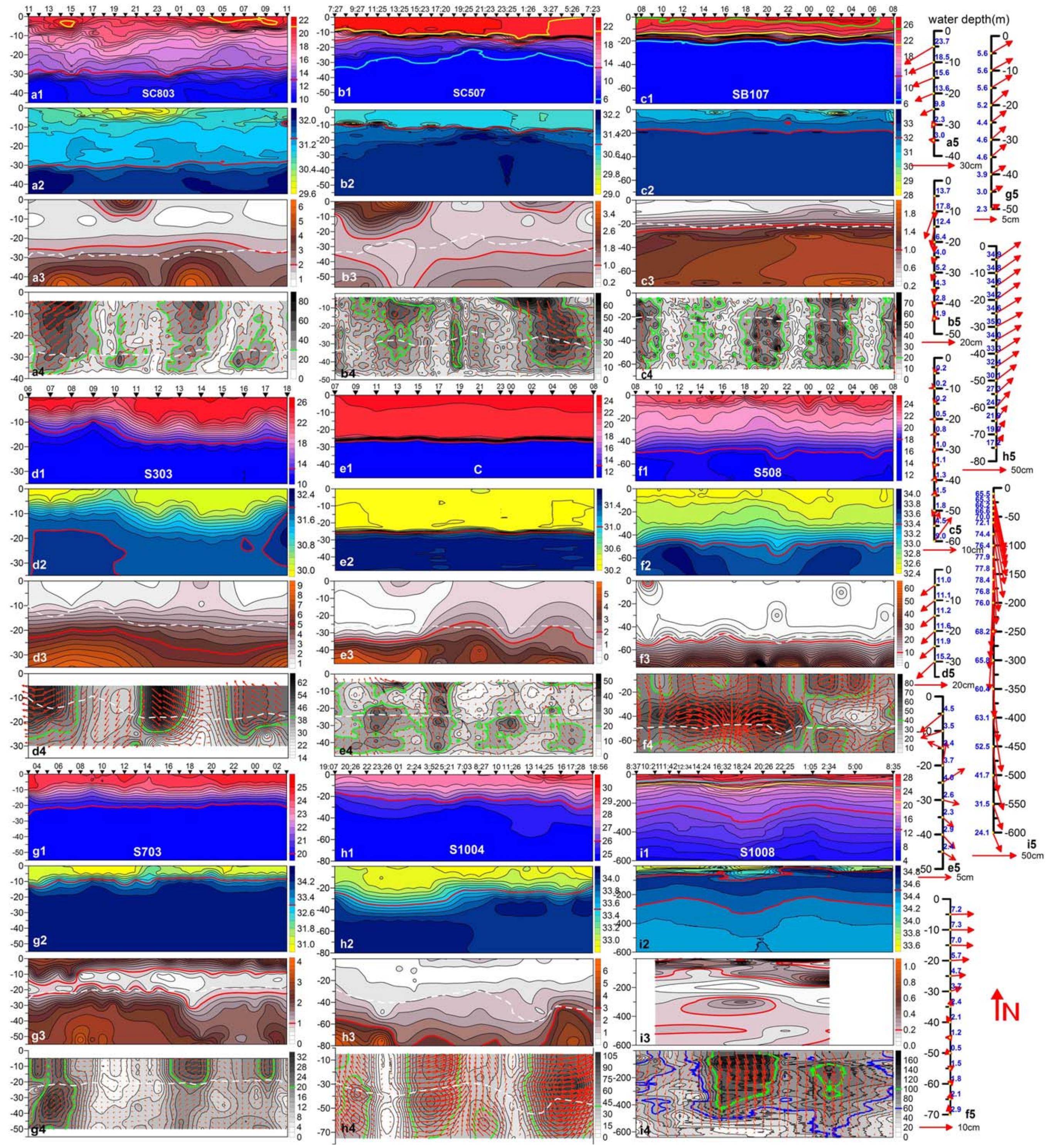

Figure 7. Continuous observation stations of the ECSs in summer, 2006. (a) Station SC803, observation beginning at 11:00, 30 July 2007 for 25 h at 1 h interval; a1–a5 are temperature (°C), salinity (*psu*), SSC (mg/L), tidal current (cm/s), and residual current (cm/s). (b) Station SC507, observation beginning at 07:27, 27 July 2007 for 25 h at 1 h interval; (c) station SB107, observation beginning at 07:31, 5 August 2006 for 25 h at 1 h interval; (d) station S303, observation beginning at 06:00, 15 July 2007 for 13 h at 1 h interval; (e) station C, observation beginning at 07:00, 9 September 2005 for 13 h at 1 h interval; (f) station S508, observation beginning at 09:00, 12 July 2006 for 25 h at 1 h interval; (g) station S703, observation beginning at 03:00, 5 July 2006 for 25 h at 1 h interval; (h) station S1004, observation beginning at 19:07, 28 June 2006 for 25 h at 1 h interval; (i) station S108, observation beginning at 08:37, 30 June 2006 for 25 h at 1 h interval. The broken line indicates the top boundary of the cold water.

Due to the supply of the NSCC, the SSC in the CWM bottom of the northern ECS exceeded 30 mg/L, and had been controlled by the thermocline.

Continuous station S508 at the southern edge of the CWM showed that thermocline and halocline were well developed at the depth of 50 m with higher SSC of >30 mg/L. Residual current above the thermocline flowed eastward at an average speed of 6 cm/s. Weak residual current inside the CWM flowed northward with an average speed of 2 cm/s. S703 was a key station at the south Changjiang estuary, and showed that the high temperature, low salinity, and high SSC occurred in the upper 10 m layer as a typical feature of the Changjiang diluted water. Below 25 m depth, the salinity and temperature were low, but the SSC was high. The suspended sediment was trapped by the CWM with a weak residual current of 4.5 cm/s. Station S1004 was similar to S703 in temperature, salinity, SSC and current direction, but appeared stronger residual current about 30 cm/s from Taiwan Strait (supporting information Figure S6). Station S1008 near the edge of the Okinawa Trough appeared strong residual current toward south with the average speed of 71 cm/s above 400 m depth. According to the direction of the Kuroshio axis, a strong eddy also occurred there, where the surface desalination and SSC were high. Above observations showed that the cold water in central and south ECS was different from the CWM of the YS. This cold water was a sediment trap, but the tidal current and residual current had been not influenced by the thermocline. In the CWMs of south YS and north ECS, the current direction and speed were not coincident between two layers of above and below the thermocline.

3.4. Autumn in 2007 (Figures 8, 9 and Supporting Information Figures S7 and S8)

3.4.1. Yellow Sea

The CWM occurred also in the YS, but its range was obviously reduced, and the thermocline and halocline fell to 40 m depth. The higher SSC was still controlled by the CWM. The coastal current brought more sediment along the SPCC, where the SSC could exceeded 30 mg/L. Low salinity and high SSC near stations F405 and F406 had indicated the continued existence of the NSCC, which was still extending to the ECS. Continuous station F308 had been measured inside the CWM, where the suspended sediment was restricted under the thermocline. The distribution of the high SSC was obviously influenced by the tidal current change. Above the thermocline, residual current was strong with the average speed of 10.3 cm/s flowing to southeast. Below the thermocline, residual current was weak and flowing to east by north at 3.5 cm/s. This current structure could cause a velocity shear layer inside the thermocline and halocline, and then trap suspended sediment into the CWM. The appearance of anomaly cool layer of 5 m thick below the thermocline at the temperature profile of F308 could be attributed to the shear. Similar feature can be found in the salinity interbed of C1004 (supporting information Figure 5b2).

3.4.2. East China Sea

Profiles [5] and [6] showed that the Kuroshio flowed northward, which was also confirmed by high temperature in the east profile [4]. Meantime, the YS was invaded by the warm current (supporting information Figure S8b). The water climbing below the Kuroshio into the shelf appeared clearly based on the temperature and salinity of profile [6]. On profile [Fj1], the thermocline covering the CWM shrank to 60 m depth with the SSC of more than 20 mg/L. From the temperature, salinity and SSC of profile [7], it was clear that the ZMCC began to develop in this season, resulting in the low temperature, low salinity and high SSC. Because of the disappearance of CWM, the changes of temperature, salinity and current presented vertically uniform in continuous stations F508 and F1004. The residual currents flowed northeast at an average speed of 16 cm/s (F1004). In station F508, the residual current reached 6.5 cm/s, and its SSC change was closely relationship with the velocity of tide current.

4. Discussion

Based on above comprehensive analysis of survey and monthly averaged data, it is clear that all changes on marine circulation, suspended sediment diffusion and CWM in the ECSs appear seasonality [*Chern et al*., 1990; *Shi and Wang*, 2010]. After comparing with the monthly averaged temperature, salinity, and current, our measured profiles have representativeness for four seasons. The spring and autumn appear merely the continuation or transition of the winter and summer. Based on systematic analysis of our survey data, monthly averaged hydrological data (supporting information Figures S1–S8) and previous studies [*Li et al*., 2006, *Liu et al*., 2006, 2007; *Yuan and Hsueh*, 2010; *Zhou et al*., 2015], we can divide the marine circulation

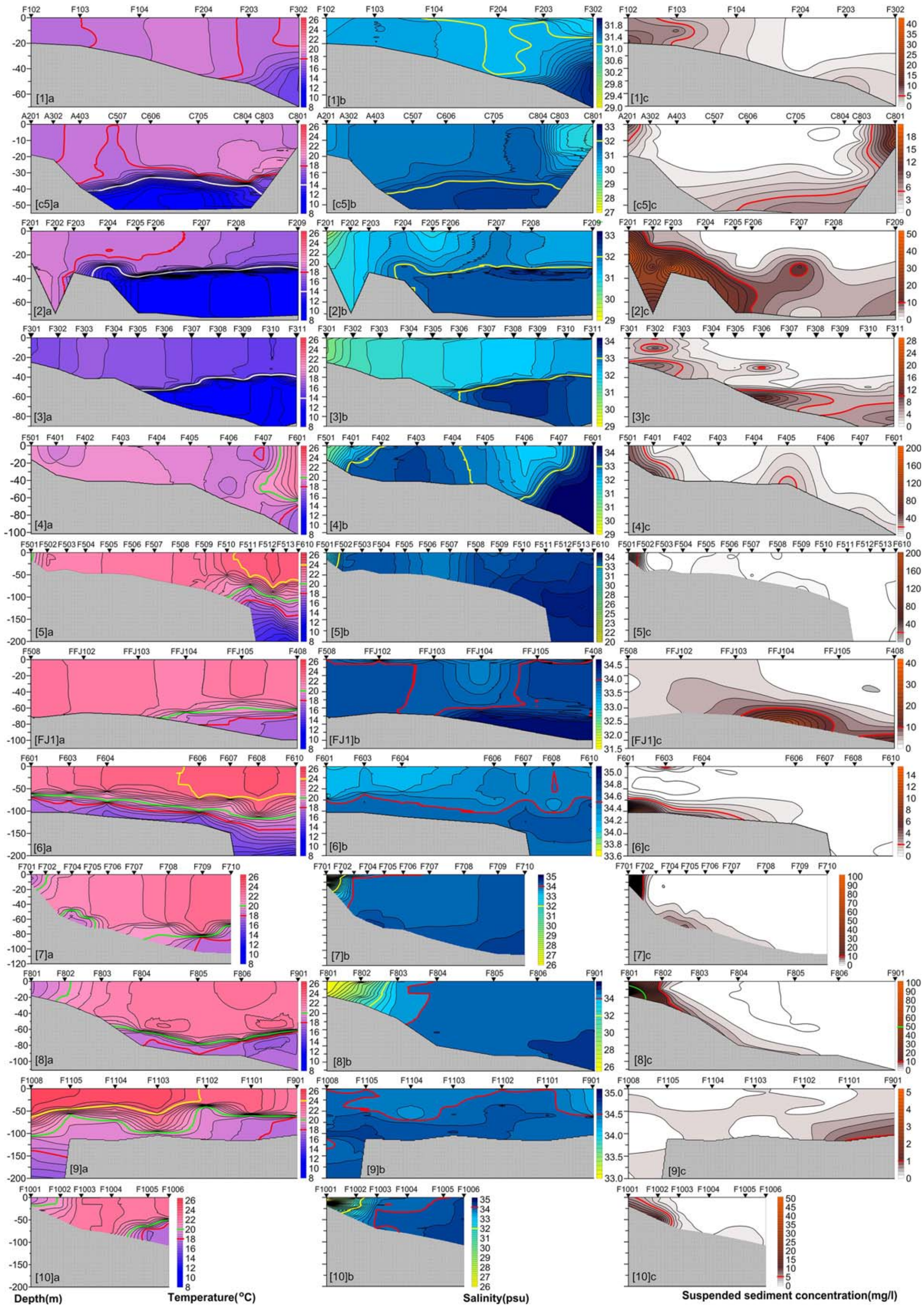

Figure 8. Observation profiles of the ECSs in autumn, 2007. [1] to [10] denote the number of profiles; a, b, c, are temperature (°C), salinity (*psu*), and the SSC (mg/L).

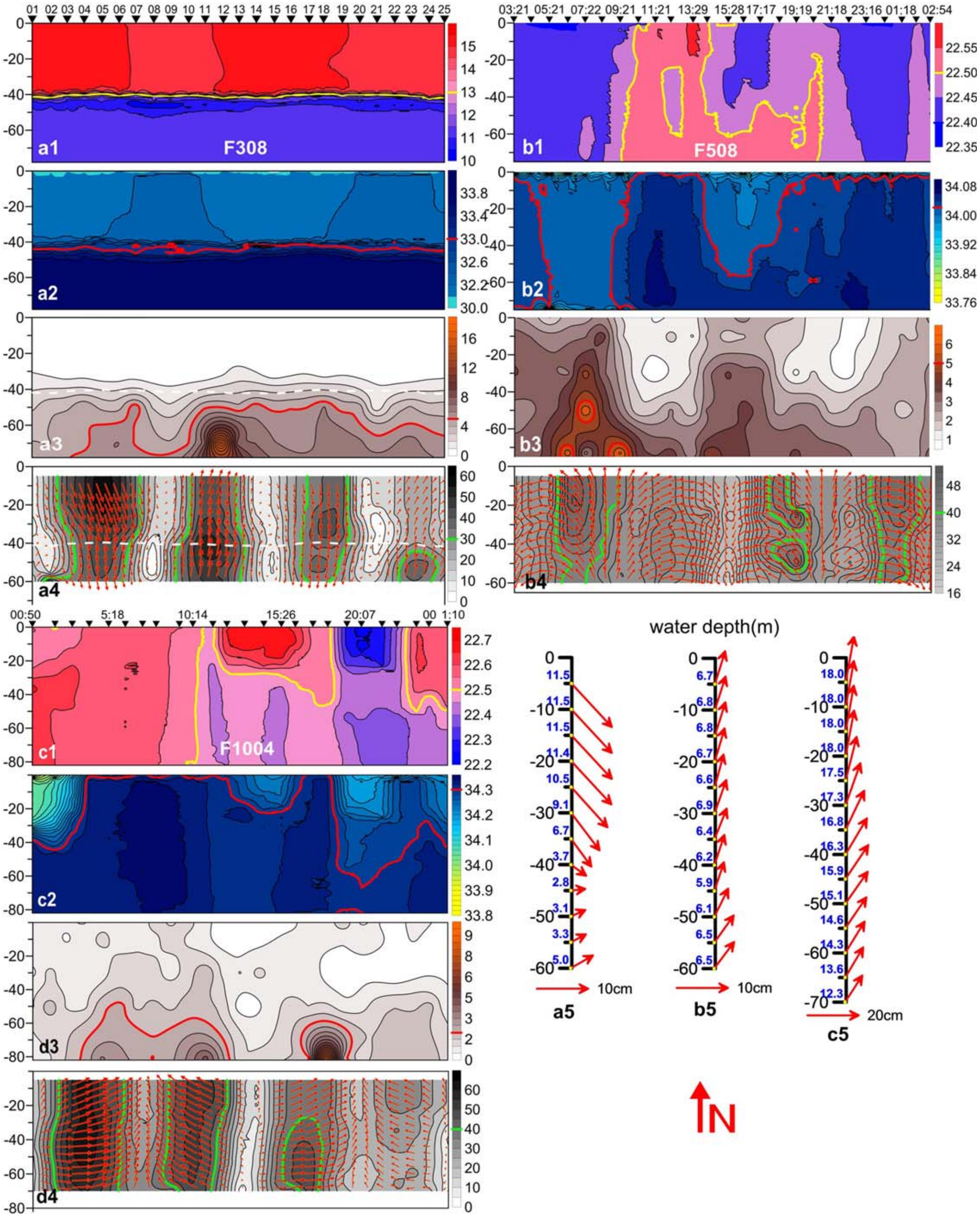

Figure 9. Continuous observation stations of the ECSs in autumn, 2007. (a) Station F308, observation beginning at 01:00, 23 November 2007 for 25 h at 1 h interval; a1–a5 are temperature (°C), salinity (*psu*), SSC (mg/L), current speed (cm/s), and residual current (cm/s). (b) Station F508, observation beginning at 03:21, 8 November 2007 for 25 h at 1 h interval; (c) station F1004, observation beginning at 00:51, 15 November 2007 for 25 h at 1 h interval. The broken line indicates the top boundary of the CWM.

and suspended sediment diffusion in the ECSs into two patterns (Figure 10), one is winter-half-year from about October to the following April, and the other is summer-half-year from about May to September.

4.1. Sedimentary Dynamics Pattern in Winter-Half-Year

In winter-half-year, solar radiation is weakening and winter monsoon strengthening, resulting in strong vertical mixing of the seawater [*Shi and Wang*, 2010]. Stratification of seawater is not prominent, and the circulation structure appears relatively uniform in vertical.

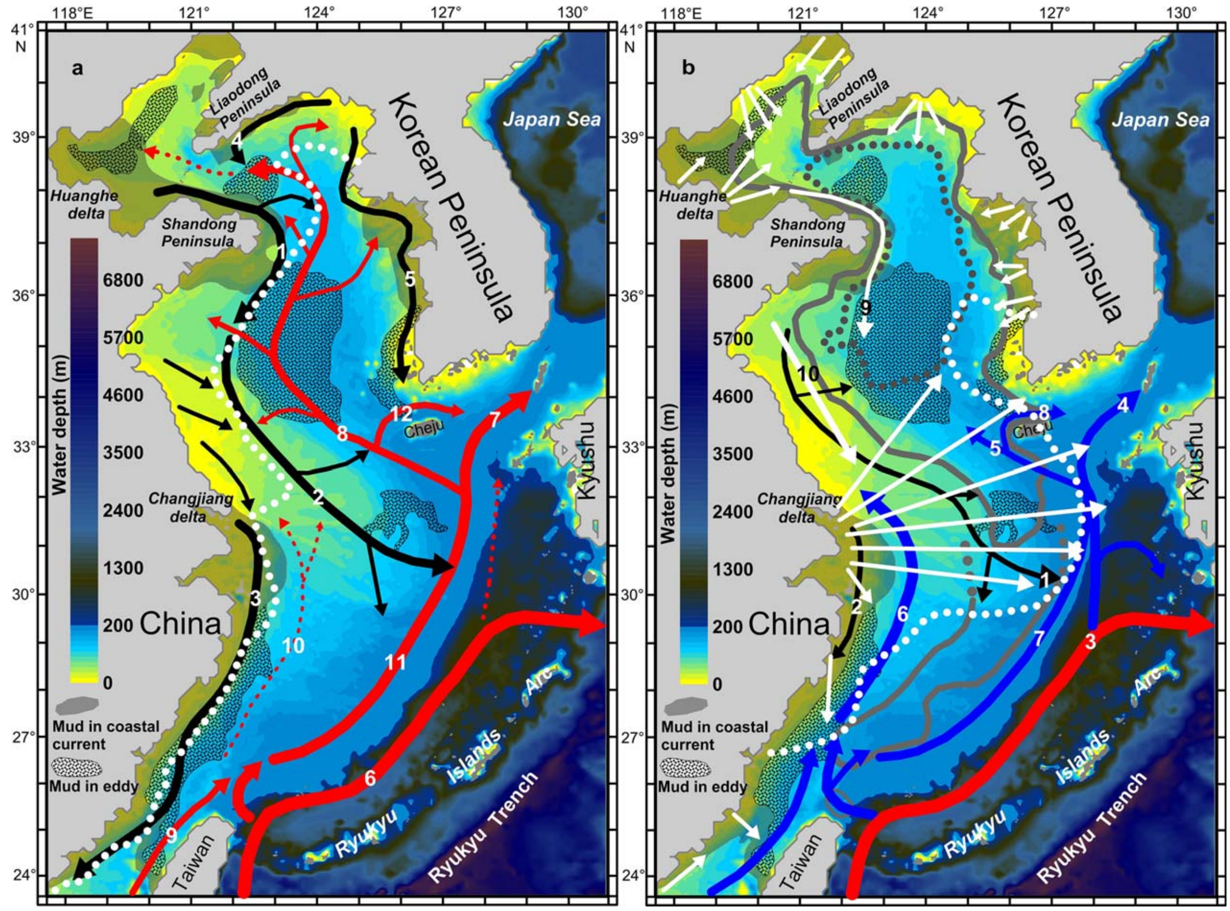

Figure 10. Sedimentary dynamics patterns in the YS and ECS. (a) The pattern of winter-half-year. The black lines indicate the coastal current systems. They are the channel for suspended sediment transport and deposition. White dot line is the diluted water boundary of salinity 32 *pus*. The red lines indicate the warm current systems which barely carry the suspended sediment. Number 1, SPCC. 2, NSCC. 3, ZMCC. 4, coastal current off the Liaodong Peninsula. 5, coastal current off the Korea Peninsula. 6, Kuroshio. 7, Tsushima warm current. 8, YSWC. 9, Taiwan Strait warm current. 10, weak TWC in the lower layer. 11, the shelf edge current of the ECS. 12, Cheju warm current. Other thin lines are the branches from the main current. (b) The pattern of summer-half-year with obvious vertical stratification. In the middle and lower water layer: number 1, NSCC. 2, coastal diffusion off the Changjiang estuary. 3, Kuroshio above 200m water depth. 4, Tsushima warm current. 5, YSWC. 6 and 7, TWC and the shelf edge current of the ECS, respectively, in whole water body. 8, Cheju warm current. Based on the distribution of temperature, salinity and currents in supporting information Figures S5 and S6 and our measured data, the CWM is distinguished. A biggest CWM is circled by a gray line along about 15°C isothermal line in the YS and north ECS. The area circled by the gray dot line along the 10°C isothermal line is the CWM core in the YS. In the upper water layer: number 9, SPCC. 10, NSCC. White dot line is the diluted water boundary of salinity 32 *pus*, the most prominent is the diffusion of Changjiang River plume.

The YSWC begins into the YS at October (supporting information Figure S8b). The SSC is very low in the YSWC. Observations in January show that the YSWC enters the YS from the south of Cheju Island at a speed of 10.5 cm/s, and 3.6 cm/s when reaching Bohai Strait. The average speed of the YSWC observed in middle of south YS is 5 cm/s [*Lin et al*., 2011]. This warm current has some branches characterized by relatively high temperature and salinity, such as the branch off the Qingdao coast (supporting information Figure S1) [*Lin et al*., 2011]. It blocks southward extension of the SPCC (supporting information Figures S1 and S2b). Due to proximity to the SPCC, high SSC occurs with active deposition in the northwest of south YS muddy area [*Li et al*., 2014; *Zhou et al*., 2014].

The head of the weak TWC can reach the north of Changjiang River estuary in the middle and low water layers and is correlated with deep trough topography off the estuary [*Yuan and Hsueh*, 2010]. The current is mainly derived from the Taiwan Strait and Kuroshio diffusion in the shelf edge, especially from the bend of Kuroshio in northeast of Taiwan. These results are in consistent with *Chen*'s conclusions [2011]. The simulation study by *Isobe and Beardsley* [2006] also showed that there is the Kuroshio eddy in the shelf edge all over the year and they found that the annually averaged onshore-transport of Kuroshio along the shelf break is 0.85 Sv. Although there is warm current through the Taiwan Strait, we could not see its connection with the TWC on the entrance profile [10]. The warm current from the strait may move around the Taiwan and is mixed by the Kuroshio diffusion water (supporting information Figure S2) [*Yuan et al*., 2008]. The

TWC brings very low SSC and opposite direction to the ZMCC, blocking the most of suspended sediment to be deposited in the ZMCC.

Due to the seasonal change of the East Asian monsoon, coastal current with low temperature, low salinity, and high SSC is developed. According to monthly averaged temperature, salinity, and current, the Korea coastal current and Cheju warm current occur, which were not observed directly in our survey. Coastal current off the Liaodong Peninsula is visible on the profiles of north YS. The SPCC come from Bohai Sea with high SSC, and the Yellow River is the main source of suspended sediment [*Yang et al.*, 2003]. Due to obstructing of the warm current branch of the YSWC off Qingdao coast, large amount of sediment from modern Yellow River is deposited along the SPCC, and results in large sedimentary thickness in northwest of south YS mud area [*Zhou et al.*, 2015]. The NSCC is mainly originated from old Yellow River delta. It is the third largest sediment source behind the Yellow River and Changjiang River estuaries [*Saito et al.*, 1999; *Yang et al.*, 2003]. This current moves to north ECS along the 50 m isobath. The suspended sediment carried by the NSCC is the main sediment source for the mud area of north ECS, which may be transported into north Okinawa Trough [*Shi and Wang*, 2010]. Based on our observations and monthly averaged hydrological status, the NSCC often has a branches diffusing to the YS, especially toward Cheju Island. Suspended sediment is transferred by the YSWC to form the muddy area off South Korea coast. This process has also been discovered by *Lim et al.* [2007] based on the deposition rate. Like previous studies [*Li et al.*, 2006; *Yuan and Hsueh*, 2010; *Wang et al.*, 2011], we also found that a small branch of the NSCC crossing the Changjiang River estuary enters the Zhejiang-Fujian coast. However, the suspended sediment of the ZMCC has been mainly originated from the Changjiang River outflow [*Liu et al.*, 2006; *Xu et al.*, 2009, 2012] and then extend to the Taiwan Strait [*Huh et al.*, 2011]. The high SSC of the ZMCC should results in the development of the mud zone off Zhejiang-Fujian coast in this period.

4.2. Sedimentary Dynamics Pattern in Summer-Half-Year

The circulation and sedimentation seem more complicated than in winter-half-year because of stratification under the strong solar radiation and weak summer monsoon. The circulation and suspended sediment diffusion in the upper and lower layers are very different [*Lie et al.*, 2003; *Shi and Wang*, 2010].

4.2.1. Lower Water Layer

A prominent feature is the CWM appearing. As solar radiation increasing, the CWM begins to appear in May in the YS (Figure 4). The CWMs of the YS, north ECS and Bohai Sea (supporting information Figure S5a3) are linked as a whole. The cold water of north YS is a product of cooled residual water of the YSWC. The cold water of south YS comes from several sources, mostly from cooled coastal current and YSWC (profile [3] in Figure 3). The CWM of north ECS is likely resulted from mixed NSCC. The CWM has strong ability to trap sediment, suggesting that mud area of CWM has been mainly formed in the summer. Our observations show that the sediment in CWM mud areas of south YS and north ECS mostly come from the NSCC. There is no sustained north wind during this period. Why the NSCC still exists? We believe that it is largely resulted from the tidal wave movement driven by the topography of the YS and the Coriolis force. The shoal topography off the Changjiang River estuary makes the NSCC turn southeast. The suspended sediment carried by the NSCC can reach the north Okinawa Trough [*Jiang et al.*, 2011]. The distribution of temperature, salinity, and current (supporting information Figures S5 and S6) indicates that there is a weak YSWC entering the YS trough [*Lie et al.*, 2001], and then turn into Cheju Strait.

The bottom cool water occurs in middle shelf of the ECS. Although its temperature is much higher than the CWM of the YS, the thermocline and halocline occur obviously. Supporting information Figures S5 and S6 show that the cool water comes from the climbing under the Kuroshio at the northeast Taiwan eddy [*Chern et al.*, 1990; *Chen*, 2011]. The shelf edge current of the ECS, which occur almost in four seasons, has been largely attributed to this eddy. Meanwhile, the suspended sediment from the Changjiang River is still transported southward along the coast in measured profiles. A weak CWM nearby station S1006 has been measured. The profile [10] shows that the CWM comes from the Okinawa Trough. In this CWM, no mud area has been deposited [*Li et al.*, 2014], which may be due to lack of sediment supply and even being erosion in winter-half-year.

4.2.2. Upper Water Layer

This layer appears high temperature and low salinity in the whole sea. The range of the Changjiang diluted water reaches the Tsushima Strait and north Okinawa Trough [*Lie et al.*, 2003]. *Pang et al.* [2011] also confirmed that the suspended sediment diffusion from the Changjiang diluted water can affect the south YS and ECS continental shelf, or directly reach the mud area of South Korea coast. Measurement profiles show that the diluted water of the ECSs is also transporting the suspended sediment for CWM trapping.

5. Conclusions

Our results show that the coastal current and surface diluted water are the main channel for transportation of suspended sediment. The Kuroshio and its derived warm current branches play the important role of the continental shelf circulation system and control the diffusion of suspended sediment. High SSC has been concentrated in coastal current and CWM. Based on survey data and monthly averaged hydrological status, we have identified two dynamic sedimentary patterns.

The winter-half-year pattern occurs from October to next April. The NSCC, ZMCC, and SPCC have been well developed, and are the channel for diffusion and deposition of suspended sediment along the route of coastal current. The YSWC and TWC block the suspended sediment diffusion across the shelf and promote the suspended sediment trapping along the coastal zone. The summer-half-year pattern appears from May to September. Water is clearly stratified due to diluted water and thermocline. A large CWM distributed in the Bohai Sea, YS and north ECS, is connected internally. The CWM has a unique role in trapping suspended sediment and can strictly limit the SSC under the thermocline and halocline. This is the main period for deposition of the CWM mud area, when the NSCC is still the major supplier of suspended sediment. We believe that the cool water at the bottom of the ECS is resulted from the water climbing of the Okinawa Trough. The surface layer has been occupied by the diluted water with low salinity, high temperature in the ECS, especially from the Changjiang River outflow. The diffusion range of suspended sediment can reach the Okinawa Trough and South Korea coast.

The NSCC and ZMCC are the main suppliers of suspended sediment for south YS and ECS. The NSCC of summer-half-year has been formed probably due to tide and the topographic effect. Based on the measurement data, we suggest that higher CWM density under low temperature and high salinity results in weaken tidal current and residual current, and thus traps the suspended sediment under the thermocline and halocline. A strong eddy of Kuroshio edge in northeast Taiwan and a strong current along the shelf edge occur almost all seasons, which play a very important role in water exchange between ECS and the Okinawa Trough. However, these results are preliminary due to our surveys in different year, and further seasonal changes and underlying mechanisms need to be studied in the future.

Acknowledgments
We are grateful to the anonymous reviewers for their inspiring and constructive comments, which are helpful in improving the research. The currents data are available at http://tds.hycom.org/thredds/GLBu0.08/expt_19.1.html. Historical temperature and salinity data are obtained from Tianjin International Ocean information Center, China (chongjinxu@vip.163.com). Seasonal survey data in this paper are collected and managed by Ocean University of China. The processed survey data used to construct figures in this work will be made accessible by requisition through email (estuary@ouc.edu.cn). Any users of this data are required to clearly acknowledge the support of Ocean University of China. This study was supported by the National Natural Science Foundation of China (grants 41030856, 40906025 and 41476030) and the Project of Taishan Scholar.

References

Barnes, S. (1964), A technique for maximizing details in numerical weather map analysis, *J. Appl. Meteorol., 9*(*3*), 396–409.
Barnes, S. (1973), Mesoscale objective map analysis using weighted time-series observations, NOAA Tech. Memo. ERL NSSL-62, National Severe Storms Laboratory, Norman, Okla.
Chang, P. H., and A. Isobe (2003), A numerical study on the Changjiang diluted water in the Yellow and East China Seas. *J. Geophys. Res.*, *108*(C9), 3299, doi:10.1029/2002JC001749.
Chang, Y. L., L. Y. Oey, C. R. Wu, and H. F. Lu (2010), Why are there upwellings on the northern shelf of Taiwan under northeasterly winds?, *J. Phys. Oceanogr.*, *40*, 1405–1417.
Chen, C. T. A. (2011), Downwelling then upwelling again of the upwelled Kuroshio water in the southern East China Sea, *J. Geophys. Res.*, *116*, C07003, doi:10.1029/2011JC007030.
Chen, C. T. A., and S. L. Wang (2006), A salinity front in the southern East China Sea separating the Chinese coastal and Taiwan Strait waters from Kuroshio waters, *Cont. Shelf Res.*, *26*, 1636–1653.
Chen, Q. Q., and Y. R. Zhu (2012), Holocene evolution of bottom sediment distribution on the continental shelves of the Bohai Sea, Yellow Sea and East China Sea, *Sediment. Geol.*, *273–274*, 58–72.
Chern, C. S., J. Wang, and D. P. Wang (1990), The exchange of Kuroshio and East China Sea shelf water. *J. Geophys. Res.*, *95*(C9), 16,017–16,023.
Dong, L. X., W. B. Guan, Q. Chen, X. H. Li, X. H. Liu, and X. M. Zeng (2011), Sediment transport in the Yellow Sea and East China Sea, *Estuarine Coastal Shelf Sci.*, *93*, 248–258.
Fischer, J., and V. Martin (1993), Deep velocity profiling with self-contained ADCPs, *J. Atmos. Ocean Technol.*, *10*(*10*), 764–773.
He, C. B., Y. X. Wang, Z. Y. Lei, and S. Xu (1959), A preliminary study on the generation and the characteristics of the Cold Water Mass of the Yellow Sea (with English abstract), *Oceanol. Limnol. Sin.*, *2*, 11–15.
Huh, C. A., W. F. Chen, F. H. Hsu, C. C. Su, J. K. Chiu, S. Lin, C. S. Liu, and B. J. Huang (2011), Modern (>100 ears) sedimentation in the Taiwan Strait: Rates and source-to-sink pathways elucidated from radionuclides and particle size distribution, *Cont. Shelf Res.*, *31*, 47–63.
Ichikawa, H., and M. Chaen (2000), Seasonal variation of heat and freshwater transports by the Kuroshio in the East China Sea, *J. Mar. Syst.*, *24*, 119–129.
Isobe, A., and R. C. Beardsley (2006), An estimate of the cross-frontal transport at the shelf break of the East China Sea with the Finite Volume Coastal Ocean Model, *J. Geophys. Res.*, *111*, C03012, doi:10.1029/2005JC003290.
Isobe, A., M. Ando, T. Watanabe, T. Senjyu, S. Sugihara, and A. Manda (2002), Freshwater and temperature transports through the Tsushima-Korea Straits. *J. Geophys. Res.*, *107*(C7), 3065, doi:10.1029/2000JC000702.
Jiang, F. Q., A. C. Li, and T. G. Li (2011), Sediment pathway of the East China Sea inferred from an R-mode factor analysis of surface sediments in the Okinawa Trough, *Quat. Int.*, *230*, 13–20.
Li, G. X., X. B. Han, S. H. Yue, G. Y. Wen, R. M. Rongmin, and T. M. Kusky (2006), Monthly variations of water masses in the East China Seas, *Cont. Shelf Res.*, *26*, 1954–1970.

Li, G. X., P. Li, Y. Liu, L. L. Qiao, Y. Y. Ma, J. S. Xu, and Z. G. Yang (2014), Sedimentary system response to the global sea level change in the East China Seas since the last glacial maximum, *Earth Sci. Rev.*, *139*, 390–405.

Lie, H. J. (1986), Summertime hydrographic features in the southeastern Hwanghae, *Prog. Oceanogr.*, *17*, 229–242.

Lie, H. J., C. H. Choi, J. H. Lee, S. Lee, and Y. Tang (2000), Seasonal variation of the Cheju Warm Current in the northern East China Sea, *J. Oceanogr.*, *56*, 197–211.

Lie, H. J., C. H. Cho, J. H. Lee, S. Lee, Y. X. Tang, and E. M. Zou (2001), Does the Yellow Sea Warm Current really exist as a persistent mean flow?, *J. Geophys. Res.*, *106*(C10), 22,199–22,210.

Lie, H. J., C. H. Cho, J. H. Lee, and S. Lee (2003), Structure and eastward extension of the Changjiang River plume in the East China Sea, *J. Geophys. Res.*, *108*(C3), 3077, doi:10.1029/2001JC001194.

Lim, D. I., J. Y. Choi, H. S. Jung, K. C. Rho, and K. S. Ahn (2007), Recent sediment accumulation and origin of shelf mud deposits in the Yellow and East China Seas, *Prog. Oceanogr.*, *73*, 145–159.

Lin, X. P., J. Y. Yang, J. S. Guo, Z. X. Zhang, Y. Q. Yin, X. Z. Song, and X. H. Zhang (2011), An asymmetric upwind flow, Yellow Sea Warm Current: 1. New observations in the western Yellow Sea, *J. Geophys. Res.*, *116*, C04026, doi:10.1029/2010JC006513.

Liu, J., Y. Saito, X. H. Kong, H. Wang, L. H. Xiang, C. Wen, and R. Nakashima (2010), Sedimentary record of environmental evolution off the Yangtze River estuary, East China Sea, during the last w13,000 years, with special reference to the influence of the Yellow River on the Yangtze River delta during the last 600 years, *Quat. Sci. Rev.*, *29*, 2424–2438.

Liu, J. P., A. C. Li, K. H. Xu, D. M. Velozzi, Z. S. Yang, J. D. Milliman, and D. J. DeMaster (2006), Sedimentary features of the Yangtze River-derived along-shelf clinoform deposit in the East China Sea, *Cont. Shelf Res.*, *26*, 2141–2156.

Liu, J. P., K. H. Xu, A. C. Li, J. D. Milliman, D. M. Velozzi, S. B. Xiao, and Z. S. Yang (2007), Flux and fate of Yangtze River sediment delivered to the East China Sea, *Geomorphology*, *85*, 208–224.

Ma, J., F. L. Qiao, C. S. Xia, and C. S. Kim (2006), Effects of the Yellow Sea Warm Current on the winter temperature distribution in a numerical model, *J. Geophys. Res.*, *111*, C11S04, doi:10.1029/2005JC003171.

Martin, V. (2002), Deep velocity profiling using lowered acoustic Doppler current profilers: Bottom track and inverse solutions, *J. Atmos. Oceanic Technol.*, *9*(S), 794–807.

Milliman, J. D., and R. H. Meade (1983), World-wide delivery of river sediment to the oceans, *J. Geol.*, *91*, 1–21.

Pang, C. G., W. Yu, Y. Yang, and D. X. Han (2011), An improved method for evaluating the seasonal variability of total suspended sediment flux field in the Yellow and East China Seas, *Int. J. Sediment. Res.*, *26*, 1–14.

Park, S. C., H.-H. Lee, H. S. Han, G. H. Lee, D. C. Kim, and D. G. Yoo (2000), Evolution of late Quaternary mud deposits and recent sediment budget in the southeastern Yellow Sea, *Mar. Geol.*, *170*(3–4), 271–288.

Qiao, L. L., X. H. Wang, Y. Z. Wang, D. X. Wu, X. W. Bao, and L. Mu (2011a), Winter heat budget in the Huanghai Sea and the effect from Huanghai Sea Warm Current, *Acta Oceanol. Sin.*, *30*(5), 56–63.

Qiao, L. L., Y. Liu, J. J. Chen, Y. Y. Ma, G. X. Li, and J. Song (2011b), Distribution and its mechanism of suspended particulate matters in the southern Huanghai Sea and the East China Sea in summer, *Acta Oceanol. Sin.*, *30*(5), 94–100.

Qiao, L. L., Y. Z. Wang, G. X. Li, S. G. Deng, Y. Liu, and L. Mu (2011c), Distribution of suspended particulate matter in the northern BohaiBay in summer and its relation with thermocline, *Estuarine Coastal Shelf Sci.*, *93*(3), 212–219.

Saito, Y., K. Ikehara, and H. Katayama (1999), Terrigenous sediment transport to the East China Sea Shelf and the northern Okinawa Trough, in *Margin Flux in the East China Sea*, edited by D. X. Hu and S. Tsunogai, pp. 35–41, China Ocean Press, Beijing.

Shi, W., and M. H. Wang (2010), Satellite observations of the seasonal sediment plume in central East China Sea, *J. Mar. Syst.*, *82*, 280–285.

Su, J. L., and W. Wang (1987), On the sources of the Taiwan Warm Current from the South China Sea, *Chin. J. Oceanol. Limnol.*, *5*(4), 299–308.

Takikawa, T., J.-H. Yoon, and K.-D. Cho (2005), The Tsushima Warm Current through Tsushima Straits estimated from ferryboat ADCP data, *J. Phys. Oceanogr.*, *35*, 1154–1168.

Teague, W. J., and G. A. Jacobs (2000), Current observations on the development of the Yellow Sea Warm Current, *J. Geophys. Res.*, *105*(C2), 3401–3411.

Teague, W. J., G. A. Jacobs, H. T. Perkins, J. W. Book, K. I. Chang, and M. S. Suk (2002), Low-frequency current observations in the Korea/Tsushima Strait, *J. Phys. Oceanogr.*, *32*, 1621–1641.

Uda, M. (1934), The results of simultaneous oceanographic investigations in the Japan Sea and its adjacent waters in May and June, 1932. *J. Imp. Fish. Exp. Stn.*, *5*, 138–190.

Wang, H. J., Y. Saito, Y. Zhang, N. S. Bi, X. X. Sun, and Z. S. Yang (2011), Recent changes of sediment flux to the western Pacific Ocean from major rivers in East and Southeast Asia, *Earth Sci. Rev.*, *108*, 80–100.

Wang, Y. H., G. X. Li, W. G. Zhang, and P. Dong (2014), Sedimentary environment and formation mechanism of the mud deposit in the central South Yellow Sea during the past 40 kyr, *Mar. Geol.*, *347*, 123–135.

Wang, X. H., F. L. Qiao, J. Lu, and F. Gong (2011), The turbidity maxima of the northern Jiangsu shoal-water in the Yellow Sea, China, *Estuarine Coastal Shelf Sci.*, *93*, 202–211.

Xie, L. L., X. J. Xiong, Q. X. Yang, and Y. W. Zhang (2009), Parameters setting of the configure file and data processing for LADCP, *Ocean Technol.*, *28*(1), 19–23.

Xiong, X. J., B. H. Guo, and X. M. Hu (2003), Key Technology of LADCP observation and data post-processing, *Ocean Technol.*, *22*(4), 32–36.

Xu, K. H., A. C. Li, J. P. Liu, J. D. Milliman, Z. S. Yang, C. S. Liu, S. J. Kao, S. M. Wan, and F. J. Xu (2012), Provenance, structure, and formation of the mud wedge along inner continental shelf of the East China Sea: A synthesis of the Yangtze dispersal system, *Mar. Geol.*, *291–294*, 176–191.

Xu, K. H., J. D. Milliman, A. C. Li, J. P. Liu, S. J. Kao, and S. M. Wan (2009), Yangtze- and Taiwan-derived sediments on the inner shelf of East China Sea. *Cont. Shelf Res.*, *29*, 2240–2256.

Yang, S. Y., H. S. Jung, D. I. Lim, and C. X. Li (2003), A review on the provenance discrimination of sediments in the Yellow Sea, *Earth Sci. Rev.*, *63*, 93–120.

Yuan, D. L., and Y. Hsueh (2010), Dynamics of the cross-shelf circulation in the Yellow and East China Seas in winter, *Deep Sea Res., Part II*, *57*, 1745–1761.

Yuan, D. L., J. R. Zhu, C. Y. Li, and D. X. Hu (2008), Cross-shelf circulation in the Yellow and East China Seas indicated by MODIS satellite observations, *J. Mar. Syst.*, *70*, 134–149.

Zhou, C. Y., P. Dong, and G. X. Li (2015), Hydrodynamic processes and their impacts on the mud deposit in the Southern Yellow Sea, *Mar. Geol.*, *360*, 1–16.

Zhu, Y., and R. Chang (2000), Preliminary study of the dynamic origin of the distribution pattern of bottom sediments on the continental shelves of the Bohai Sea, Yellow Sea and East China Sea, *Estuarine Coastal Shelf Sci.*, *51*, 663–680.